

# Optimal Power Flow in the Smart Grid Using Direct Load Control Program

S. Derafshi Beigvand, H. Abdi\*

Department of Electrical Engineering, Engineering Faculty, Razi University, Kermanshah, Iran

## ABSTRACT

*This paper proposes an Optimal Power Flow (OPF) algorithm by Direct Load Control (DLC) programs to optimize the operational cost of smart grids considering various scenarios based on different constraints. The cost function includes active power production cost of available power sources and a novel flexible load curtailment cost associated with DLC programs. The load curtailment cost is based on a virtual generator for each load (which participates in DLC program). To implement the load curtailment in the objective function, we consider incentive payments for participants and a load shedding priority list in some events. The proposed OPF methodology is applied to IEEE 14, 30-bus, and 13-node industrial power systems as three examples of the smart grids, respectively. The numerical results of the proposed algorithm are compared with the results obtained by applying MATPOWER to the nominal case by using the DLC programs. It is shown that the suggested approach converges to a better quality solution in an acceptable computation time.*

**KEYWORDS:** Automated demand response, Demand response, Direct load control, Load curtailment, Optimal power flow, Smart grid.

## 1. INTRODUCTION

Smart grid is a self-healing electrical network, which includes smart loads, distributed generation resources, storage devices, energy management system (EMS), communication technology, and digital calculations. In the smart grid, the network and customers become active. Generally, it is an open strategy for using the renewable and non-renewable energy resources, reducing costs, increasing reliability [1] and adding new abilities and facilities to the existing power system. This intelligent system is the result of the concomitant use of information and communication technologies in the power system.

One of the main components of the smart grid is demand response (DR) [2,3]. By introducing incentive-based schemes or price-based schemes offered by the local electric company, DR can

reduce the customer's load demands. DR is a subset of the energy consumption management defined by the U.S. department of energy (DOE) in 2006 as "Changing in the electricity consumption by the end-users in response to changes in the electricity price over time, or to incentive payments designed to induce lower electricity use at times of high wholesale market prices or when system reliability is jeopardized, from their normal consumption patterns [3]."

Automated demand response (Auto-DR) programs, enable customers to participate in the DR programs without manual intervention. Because of their advantages, customers only pre-select the level of the participation in the DR program and when an Auto-DR is implemented, an automated load control system (ALCS) will reply to the DR.

Direct load control (DLC) is a subset of incentive-based demand response in the smart grids. The DLC is a good platform to implement the load curtailment programs (demand shed strategy), allowing the network operators to directly and/or indirectly reduce the total customer demand through curtailing

customer loads.

On the other hand, most studies of the power systems are based on the optimization methods that satisfy all constraints, supply the load demand continuously, and provide a high reliability level. The main objective of the optimal power flow (OPF) study in the power systems is the power flow optimization, whilst satisfying all equality and inequality constraints in the power system and devices. The OPF studies in the smart grids, search the optimal operating point of the power system.

Recently, different OPF methodologies for smart grids have been proposed. In [4], Lin and Chen proposed a distributed and parallel OPF algorithm using a combination of Lagrange projected gradient method and recursive quadratic programming method to achieve a complete decomposition of the OPF problem into a set of sub-problems for processing units at each bus. They also dealt with the computational synchronization challenges under asynchronous data, which exist in a Petri net control model. This approach significantly reduces the computational time by considering fast variations of renewable sources. In [5], Bruno et al. proposed an unbalanced three-phase OPF for smart grids based on a quasi-Newton method to solve an unconstrained problem, iteratively. This method does not require the analytical evaluation of the first-order derivatives of the objective function, and consequently, does not need the evaluation of the Hessian of the obtained unconstrained problem. Ref. [6] proposed a distribution OPF methodology for unbalanced distribution networks. Also, Ref. [6] converts the mixed-integer nonlinear programming problem into a nonlinear programming and proposes a novel local search method. Y. Levron et al. in [7] suggested an OPF solver for smart grids by integrating the storage devices and considering the problem in both time and network domains. A main disadvantage of the proposed approach in [7] is the growth of the numerical complexity in power law with the number of different storage devices. A linear approximation of the smart microgrid was used in [8], where loads are approximated by impedances, and a semi-definite programming relaxation method was used to transfer the main non-convex problem to a convex and semi-definite

problem. In contrast to [8], Ref. [9] extended the semi-definite programming relaxation method for unbalanced systems. Ref. [10] proposed a multiphase OPF approach for unbalanced smart grids, which is useful for a detailed analysis. As reported in [5-7, 9-10], most of the related research proposed the OPF in the smart grid based on unbalanced electrical power system. In addition, these approaches do not mention the basics of the smart grid in view of customer participations in controlling the loads bilaterally via applying various strategies.

In this paper, we propose an OPF methodology for smart grids based on applying the DLC programs to optimize the active power generation cost and load curtailment cost, simultaneously. This approach converts inequality constraints into weighted equality ones, and consequently, by using a dynamic method (which will be described in section 3) finds the optimal solution while satisfying all constraints. Also, a novel load curtailment cost function was described. The main advantage of this work is associated with the participation of loads in the DR programs. In fact, DR is an open and important strategy of the demand-side management (DSM), enabling customers to control the adjustable and shedable loads and to participate in the DR programs. This action enables them to reply to the price or event signals in order to reduce their electricity usages. Also, network operators can reduce (adjust) the total demand through curtailing customer loads directly and/or indirectly.

This work is organized as follows. In section 2, we represent DR, Auto-DR and DLC programs and their effects on the smart grids. The proposed methodology is described in section 3. In section 4, numerical results in terms of quality solution and computational performances are presented on IEEE 14, 30-bus, and 13-node industrial power systems [11], where the results are compared with those obtained by MATPOWER package [12]. Finally, we draw the conclusions in section 5.

## 2. DEMAND RESPONSE IN THE SMART GRID

DR is one of the most important components of the smart grids which is a subset of the energy

consumption management. Generally, the purpose of DR is reducing the electric usage by consumers when the price of electricity in wholesale power markets is high or the system reliability has been jeopardized.

Using DR in the smart grids, will be resulted in achieving the following aims [3, 13-16]:

- Reduction of emissions in the power generation sector,
- Rectifying the imbalances caused by uncertainty in power system resources,
- Increasing the system reliability,
- Helping to remain constant the price of electricity in the market,
- Reducing the cost of power generation,
- Postponing new power plant constructions,
- Reducing the power consumption in peak load periods (peak clipping),
- Increasing the power consumption in off-peak load periods (valley filling),
- Load shifting from peak load periods to off-peak load periods,
- Reduction of power outages,
- Energy efficiency,
- Improving the energy consumption patterns of customers,
- Using DR as the energy saving (spinning system reserve).

One of the DR categories is the incentive-based demand response [16]. It is one of the available strategies for the electric companies and smart grid operators in emergency conditions that by using it, the system reliability is increased. They considered incentive payments for voluntary participation of consumers to reduce their electricity consumption in which there is no relationship between it and the price of electricity.

### 2.1. Automated demand response

By using the communication and control infrastructures in the smart grid, the demand response speed can be increased. It is so-called automated demand response where DR can be implemented automatically. Auto-DR is associated to the energy management and control system, and customer equipment controllers, directly. Also, it is

capable to respond to them within a few seconds to several minutes. Auto-DR uses communications infrastructures such as the Internet Protocol to inform the network operator programs and enables customers with ALCS to participate in DR programs. ALCS (such as EMS) is flexible enough to allow customers to pre-select their level of participation in the DR programs and participate in them automatically. Also, in response to the price signal or event signal, customers enable to reduce their electricity demand during the periods of the peak demand automatically.

### 2.2. Direct load control

DLC is a subset of incentive-based DR in smart grids [14, 16]. Electrical companies or independent system operators (ISO) use the DLC programs to control the customer electrical devices—when adjustable and shedable loads are under the control of the system dispatcher, through load control system and it includes shuts down or cycles a customer's electrical equipment on short notice—with prior notification remotely and directly and/or indirectly. When consumers participate in the DLC program, network operator and electrical company control the customer power consumption and can interrupt the customer devices when needed (reserve shortfalls arise or any event occurs).

The major advantages of the DLC program are as follows [17]:

- A way to replace a cost-effective demand-side with traditional generation,
- Load factor can be improved,
- A way to reduce financial,
- Electrical companies can be offered service options to the customer.

Incentive payments will be considered to encourage the customers for their acceptance and participation in DR programs, so that it is usually in the form of special concession tariffs or bill credits. Auto-DR technology is a good platform to implement the DLC programs such as load curtailment programs (demand shed strategy). Fig. 1 shows the automatic implementation of load curtailment programs by using the DLC based on Auto-DR technology [18].

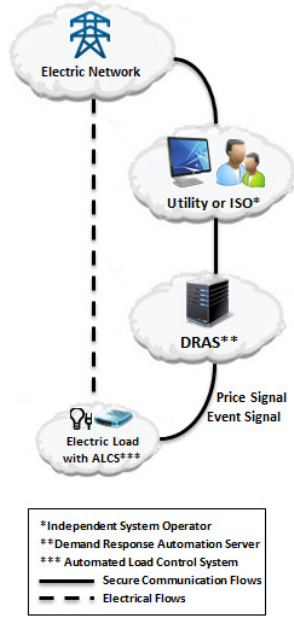


Fig. 1. Using DLC based on Auto-DR [18].

### 3. PROBLEM FORMULATION

#### 3.1. OPF formulation

The OPF problem mainly concerns with the fuel cost minimization. It contains the objective function subject to satisfy different constraints. Generally, the OPF formulates as follows:

$$\begin{aligned} & \min G(\mathbf{X}) \\ & \text{subject to } \begin{cases} \mathbf{E}(\mathbf{X}) = 0 \\ \mathbf{I}(\mathbf{X}) \leq 0 \end{cases} \end{aligned} \quad (1)$$

where  $G$  is the objective function to be optimized;  $E$  denotes the equality constraints such as power balance equations and  $I$  represents the inequality ones such as operational/capacity limits on the different units in the power system and etc;  $\mathbf{X} = [x_1, x_2, \dots, x_n]$  is the state and control variables where  $n$  is the dimension of the matrix  $\mathbf{X}$ , and  $X_{min} \leq X \leq X_{max}$ ; it should be noted that  $G$ ,  $E$ , and  $I$  are differentiable real-valued functions. Matrices and vectors represent in bold, e.g.  $\mathbf{X}$ .

In this paper, the objective function is related to two functions as follows:

1) Fuel cost function of the thermal generators: Quadratic fuel cost of generating units is function of active power production and given by

$$\sum_{i=1}^{N_g} (\alpha_i P_{gi}^2 + \beta_i P_{gi} + \gamma_i) \quad (2)$$

where  $P_{gi}$  denotes the real power generation of  $i$ th units and  $\alpha_i$ ,  $\beta_i$ , and  $\gamma_i$  are its coefficients;  $N_g$  represents the total number of generator units.

2) Cost function of the load curtailments: If we consider the minimization of the active power generation cost, only, the best result is the use of maximum load curtailments. But, this program has additional costs which should be returned to customers, finally by using special concession tariffs or bill credits. Suppose that several customers will be participated in the DLC program and there is a virtual generator for each of them so that it supplies its corresponding customer from 0 per-unit to the maximum acceptable load curtailment. In fact, each virtual generator supplies the curtailed load as shown in Fig. 2. In other words, each load demand in the DLC program will be fed through the network (for actual power load) and virtual units (for the curtailed demand) so that they supply completely.

Therefore, the load curtailment cost will be modeled as the active power generation cost of the virtual generators as follows:

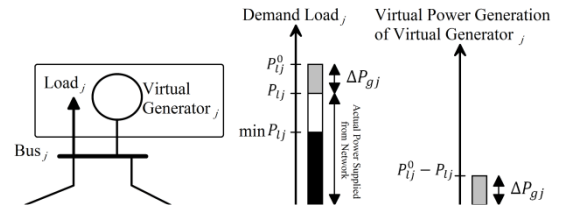


Fig. 2. Idea of the virtual generators.

$$\sum_{j \in LC} (\alpha_{lj} \Delta P_{gj}^2 + \beta_{lj} \Delta P_{gj}) \quad (3)$$

where

$$\Delta P_{gj} = P_{lj}^0 - P_{lj}$$

and where  $P_{lj}^0$  is the initial active power demand of the  $j$ th load;  $P_{lj}$  is the active power supplied to the  $j$ th curtailable load;  $LC$  denotes the set of curtailable loads;  $\alpha_{lj}$  and  $\beta_{lj}$  are the virtual generator cost coefficients.

The proposed load curtailment cost has three advantages: a) customers participate in the DR programs. In fact, in this paper, load curtailment can be implemented through the objective function; b) modeling the costs of the demand shed; In other words, incentive payments for participations. c) and

finally, in the same conditions and some events, a priority list can be implemented. On the other words, Eq. (3) will be resulted in determining the time shedding sequence of the loads (see section 4.2). It should be noted that the constant term in Eq. (3) is deleted as the payments should be considered only if the customers participate in the programs.

Finally, the objective function is as follows:

$$G = A \sum_{i=1}^{N_g} (\alpha_i P_{gi}^2 + \beta_i P_{gi} + \gamma_i) + \sum_{j \in LC} B_j (\alpha_{lj} \Delta P_{gj}^2 + \beta_{lj} \Delta P_{gj}) \quad (4)$$

where  $A$  and  $B_j$  are the weights on the objective function.

The equality constraints are active and reactive power balance equations for each bus, which can be represents as Eqs. (5) and (6), respectively. The inequality ones denote the capacity limits on the thermal generating units as Eqs. (7) and (8), voltage limits of the  $i$ th bus as Eq. 9, and capacity limits of virtual generators as Eq. (10).

$$P_{gi} - P_{li} = \sum_{j=1}^{N_b} |V_i| |V_j| (G_{lij} \cos \delta_{ij} + B_{lij} \sin \delta_{ij}), \quad i = 1, 2, \dots, N_b \quad (5)$$

$$Q_{gi} - Q_{li} = \sum_{j=1}^{N_b} |V_i| |V_j| (G_{lij} \sin \delta_{ij} - B_{lij} \cos \delta_{ij}), \quad i = 1, 2, \dots, N_b \quad (6)$$

$$P_{gi}^{\min} \leq P_{gi} \leq P_{gi}^{\max}, \quad i = 1, 2, \dots, N_g \quad (7)$$

$$Q_{gi}^{\min} \leq Q_{gi} \leq Q_{gi}^{\max}, \quad i = 1, 2, \dots, N_g \quad (8)$$

$$|V_i|^{\min} \leq |V_i| \leq |V_i|^{\max} \quad i = 1, 2, \dots, N_b \quad (9)$$

$$0 \leq \Delta P_{gi} \leq \Delta P_{gi}^{\max}, \quad i \in LC \quad (10)$$

where  $Q_{gi}$  and  $Q_{li}$  are reactive power generation and demand of  $i$ th bus, respectively;  $G_{lij}$  and  $B_{lij}$  represent the conductance and susceptance between the  $i$ th and  $j$ th bus, respectively;  $\delta_{ij}$  is the phase angle between bus  $i$  and bus  $j$ ;  $|V_i|$  denotes the voltage magnitude of the  $i$ th bus;  $N_b$  is the number of bus.

### 3.2. Proposed method

In this paper, an OPF methodology for smart grids based on the Lagrangian function and penalty function is proposed. By using the definition of the Lagrangian function, we can write:

$$\min \mathcal{L}(\mathbf{X}, \boldsymbol{\lambda}) \quad (11)$$

subject to:  $\mathbf{I}(\mathbf{X}) \leq 0$

where  $\mathcal{L}(\mathbf{X}, \boldsymbol{\lambda}) = G(\mathbf{X}) + \boldsymbol{\lambda}^T \mathbf{E}(\mathbf{X})$  and  $\boldsymbol{\lambda}^T = [\lambda_1, \lambda_2, \dots, \lambda_m]$  is the Lagrange multiplier corresponding to the equality constraints, and  $m$  is the total number of equality constraints;  $\mathcal{L}$  denotes the Lagrangian function;  $(\cdot)^T$  denotes transposition of  $(\cdot)$ .

By using the penalty function condition, inequality constraints can be converted to equality constraints as follows:

$$EI_i(\mathbf{X}) = \max^{s_i(I_i(\mathbf{X}))}(0, I_i(\mathbf{X})) \quad (12)$$

where

$$s_i(I_i(\mathbf{X})) = \frac{a_0 I_i^2(\mathbf{X}) + a_1 I_i(\mathbf{X}) + a_2}{a_3 I_i^2(\mathbf{X}) + a_4 I_i(\mathbf{X}) + a_5}$$

and  $EI_i$  is the equality constraint corresponding to the  $i$ th inequality constraint;  $k$  is the total number of the inequality constraints;  $s_i$  is the dynamic control parameter depends on  $\mathbf{X}$ ;  $a_0 - a_5$  are constant parameters (see appendix A).

Using Eqs. (11) and (12), we can rewrite the Lagrangian function as follows:

$$\min \mathcal{L}(\mathbf{X}, \boldsymbol{\lambda}, \boldsymbol{\mu}) \quad (13)$$

where

$$\mathcal{L}(\mathbf{X}, \boldsymbol{\lambda}, \boldsymbol{\mu}) = G(\mathbf{X}) + \boldsymbol{\lambda}^T \mathbf{E}(\mathbf{X}) + \boldsymbol{\mu}^T \mathbf{EI}(\mathbf{X})$$

and where  $\boldsymbol{\mu}^T = [\mu_1, \mu_2, \dots, \mu_k]$  is the Lagrange multiplier corresponding to the inequality constraints.

Eq. (13) is an unconstrained problem and can be solved as Eq. (14) [19]. The equilibrium point of Eq. (14) is called the minimum saddle-point. Above mentioned dynamic system can be solved by using *fsolve*( $\bullet$ ) function in MATLAB software, iteratively. The “*fsolve*” routine is basically an optimization routine that converges to a point where the residual is the minimum.

$$\begin{aligned} \frac{\partial \mathcal{L}}{\partial \mathbf{X}} &= \nabla_{\mathbf{X}} G(\mathbf{X}) + \lambda^T \nabla_{\mathbf{X}} \mathbf{E}(\mathbf{X}) \\ &+ \sum_i [\mu_i \max^{s_i(I_i(\mathbf{X}))^{-1}}(0, I_i(\mathbf{X})) \\ &\quad \times P(\mathbf{X}) \nabla_{\mathbf{X}} I_i(\mathbf{X})] = 0 \end{aligned} \quad (14)$$

$$\begin{aligned} \frac{\partial \mathcal{L}}{\partial \lambda} &= \mathbf{E}(\mathbf{X}) = 0 \\ \frac{\partial \mathcal{L}}{\partial \mu} &= \mathbf{E} \mathbf{I}(\mathbf{X}) = 0 \end{aligned}$$

where

$$\begin{aligned} P(\mathbf{X}) &= s_i(I_k(\mathbf{X})) \\ &+ s_i'(I_i(\mathbf{X})) \max(0, I_i(\mathbf{X})) \text{Ln} \max(0, I_i(\mathbf{X})) \end{aligned}$$

and where  $\nabla$  and  $(\cdot)'$  denote the first-order derivatives; Ln denotes the natural logarithm.

“*fsolve*” uses nonlinear least-squares algorithm that employs the Gauss-Newton or the Levenberg–Marquardt method [20-22].

Since there are no limits on the Lagrange multiplier corresponding to the inequality constraints, it is possible that some of the Lagrange multipliers become large and some others become small, theoretically. Large Lagrange multipliers may lead to stiffness of the third dynamic system of Eq.(14) in the search. Also, the points on the boundary of the feasible region may not reach it and some inequality constraints violated when the local minimum is on the boundary or out of the feasible region. In this condition, the convergence speed may be reduced. So, we can add a decay term to the third dynamic system of Eq.(14) as Eq.(15) [23, 24].

Fig. 3 shows the suggested approach which has the following steps:

**Step 1)** Put the data of generators, loads, buses, and transmission lines.

**Step 2)** Form the dynamic system Eq.(14) neglecting the inequality constraints.

**Step 3)** Set initial points (related to the state and control variables).

**Step 4)** Determine the saddle-point of the system.

**Step 5)** Use the *fsolve* function to solve OPF problem. In this step, the decisions about inequality constraints will be formed as it is shown in Fig. 3. Finally, the dynamic system Eq. (14) can be complete.

In other words, we propose the following steps for

all inequality constraint:

**Step 5.1)** Determine the saddle-point of the dynamic system Eq. (14) neglecting the inequality constraints.

**Step 5.2)** For upper limit of the  $i$ th inequality constraint, if  $x_i \in \mathbf{X}$  is smaller than the corresponding saddle-point, do step 5.3, else do step 5.4.

**Step 5.3)** Add a decay term Eq. (15) to the third dynamic system of Eq. (14) when the  $i$ th inequality constraint is satisfied and do not add it to the third dynamic system of Eq. (14) when the  $i$ th inequality constraint is violated.

**Step 5.4)** Add a decay term Eq. (15) to the third dynamic system of Eq. (14) for the  $i$ th inequality constraint.

**Step 5.5)** For the lower limit of the  $i$ th inequality constraint, if  $x_i \in \mathbf{X}$  is greater than the corresponding saddle-point, do step 5.3, else do step 5.4.

The decay term can be defined as follows

$$E I_i(\mathbf{X}) - \rho \mu_i = 0 \quad (15)$$

where  $\rho$  is a positive constant parameter and can be defined separately for Step 5.3 and Step 5.4. It controls how fast  $\mu_i$  is reduced.

When  $x_i$  is out of the feasible region and is far from the saddle-point (without considering the inequality constraints),  $\mu_i$  becomes very large; at the same time,  $s_i$  is large to force the  $x_i$  into the feasible region and increases the convergence speed. But, in this condition, convergence rate becomes more slowly. So, a decay term as Eq. (15) must be used to reduce the value of  $\mu_i$ . This makes that all inequality constraints are satisfied, as well as speed up the convergence rate. Therefore, we can treat the saddle-point without considering the inequality constraints as a decision parameter according to the above steps. In some condition as discussed above, there will be no decay term; because weights on the inequality constraints ( $s_i$  and third dynamic system of Eq. 14) are enough to speed up the convergence rates of them and force them into the feasible region.

**Step 6)** Print results.

#### 4. NUMERICAL RESULTS

The proposed methodology is tested on the IEEE 14 and 30-bus standard systems and 13-node industrial power system as examples of the smart grids. It

should be noted that like the other reported researches related to OPF in the smart grid, these systems are used as the basic electrical structures. Furthermore, they are equipped with the new infrastructures presented in section 2. In these three cases, all loads are modeled as constant power ones. Furthermore, the conductors and cables are modeled as  $\pi$ -equivalent circuits. Transformers are modeled as the short transmission lines.  $\rho$  is chosen  $10^5$  and  $10^7$  for step 5.3 and step 5.4, respectively. The constant parameters of  $s_i$  are given in Table 1. Acceptable voltage range is considered as 0.94-1.06 per-unit for PQ buses. Also, the voltage magnitude of PV buses is considered to have a constant value.

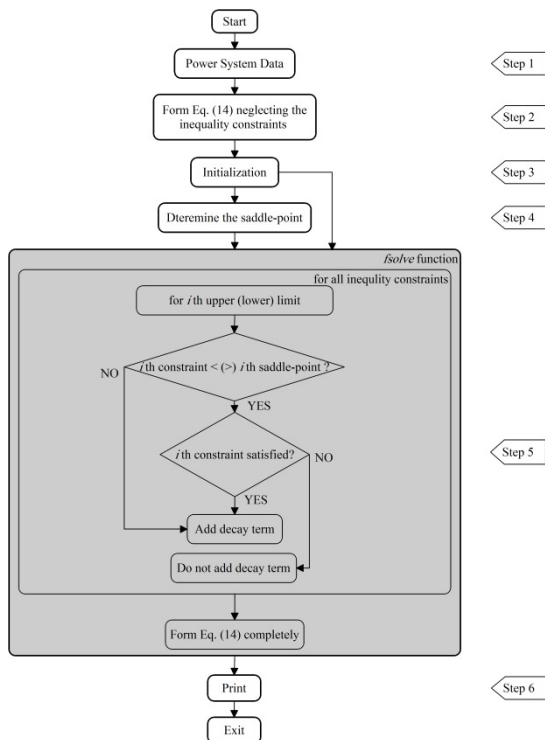


Fig. 3. Flowchart of the suggested algorithm.

The obtained solution by the suggested approach in terms of optimal operating point of the system and computational performances are compared with those obtained by MATPOWER [12] (see appendix B) for all test cases.

Table 1. Constant parameters of  $s_i$ .

$a_0$	$a_1$	$a_2$	$a_3$	$a_4$	$a_5$
2.500	-2.745	1.250	1.000	-1.497	1.000

By regulating the adjustable loads, the electricity usage can be reduced. In fact, the reduced demand

can be considered as adjustable load curtailment (adjustable demand shed). So, the variables corresponding to the load curtailment are considered as continuous variables

#### 4.1. Implementation of the DLC program and proposed methodology on IEEE 14-bus system as a smart transmission grid

IEEE 14-bus test system (Fig. 4) is a balanced and highly loaded system that has two generators and three synchronous compensators where the corresponding buses are considered as voltage controlled buses (PV buses). Generator and synchronous compensator data are given in appendix C.

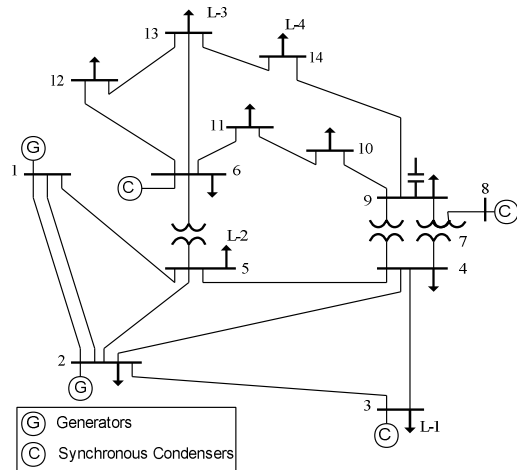


Fig. 4. IEEE 14-bus power system.

In this network, it is assumed that the customers at bus 3, 5, 13, and 14 have accepted to participate in the DLC program (load curtailment program) according to Table 2, where their power factor remains constant. In this study,  $\alpha_{lj}$  and  $\beta_{lj}$  are selected as 10 (\$/per-unit<sup>2</sup>·h<sup>-1</sup>) and 205 (\$/per-unit<sup>1</sup>·h<sup>-1</sup>) for all virtual generators, respectively.

After optimization, the value of the objective function obtained by the proposed method and MATPOWER will be equal to 133.89 and 146.12 (\$/h), respectively. Active power generation and demand by using the suggested algorithm reduced by 5.66 % and 5.44 %, respectively, in comparison with the base case (without using DLC program); but, these values for MATPOWER are 6.70 % and 6.54 %, respectively. This shows that the proposed method supplies more power demand at lower cost

in comparison with obtained results by MATPOWER (almost 1.19 %). Optimal active and reactive power generations by generators and synchronous compensators are given in Table 3.

**Table 2.** Load curtailment characteristics of IEEE 14-bus test system.

Load No.	L-1	L-2	L-3	L-4
$P_{max}^a$	0.942	0.076	0.135	0.149
$P_{min}^a$	0.850	0.040	0.077	0.100
Power Factor	0.980	0.978	0.918	0.948

<sup>a</sup>Active power demand in [per-unit].

The results of load curtailment programs are shown in Fig. 5. For the introduced algorithm, it shows that the load demand by in bus 5 (L-2) not curtailed (unlike MATPOWER result) and the L-1, L-3, and L-4 reduced by 7.37 %, 42.44 %, and 9.93 %, respectively. Fig. 6 illustrates the voltage profiles of IEEE 14-bus system with and without implementation of DLC program. As shown, both two methods satisfy the related constraints.

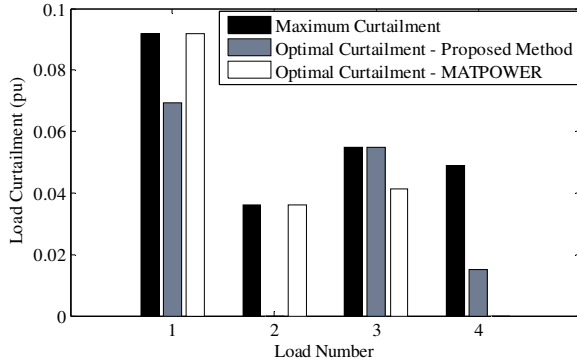


**Fig. 5.** Results of implementation load curtailment program on IEEE 14-bus system.

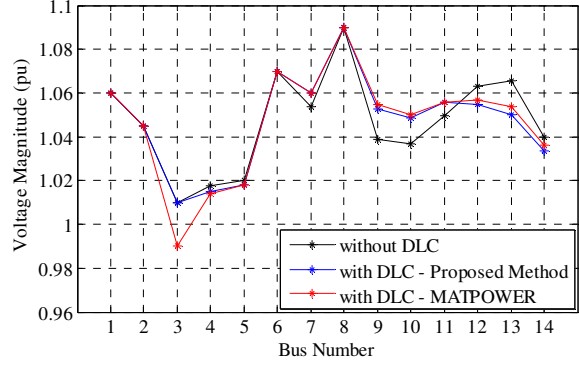


**Fig. 6.** Voltage profile of IEEE 14-bus system.

The load factors of curtailed loads are shown in Fig. 7. This figure indicates that the load factors are improved in comparison with minimum ones. It should be mentioned that the minimum load factors are calculated based on the maximum load curtailments.

**4.2. Implementation of DLC program and proposed methodology on 13-node industrial power system as a smart distribution grid**

The single-line diagram of the 13-node industrial power system is presented in Fig. 8. System data is given in appendix D. This balanced system is a part of the industrial system of [11] that has two generators. Suppose that the smart grid is in the islanded mode and some abnormal events have led to the reduction in system reserve. At the same time, connecting to the utility is not possible. For this condition, the following maximum active power generations are selected (in per-unit):  $P_{g1} \leq 0.352$ ,  $P_{g2} \leq 0.256$ . In this condition, to increase the system reliability, DLC program (demand shed strategy) is implemented. In this case, all loads have

**Table 3.** Optimal power generations of IEEE 14-bus test system.

		$P_{g1}^a$	$P_{g2}$	$Q_{g1}$	$Q_{g2}$	$Q_{g3}$	$Q_{g6}$	$Q_{g8}$	Total Cost <sup>b</sup>
Without DLC		1.799	0.901	-0.043	0.266	0.255	0.144	0.189	-
With DLC	Proposed	1.727	0.820	-0.036	0.257	0.206	0.102	0.184	133.89
	MATPOWER	1.746	0.773	-0.035	0.395	0.000	0.116	0.185	146.12

<sup>a</sup>All in [per-unit]. <sup>b</sup>All in [ $\$.h^{-1}$ ].

**Table 4.** Load curtailment characteristics of 13-node industrial power system.

Load No.	L-1	L-2	L-3	L-4	L-5	L-6
$P_{max}^a$	0.0478	0.0703	0.0963	0.1237	0.0353	0.2650
$P_{min}^a$	0.0400	0.0474	0.0850	0.1160	0.0300	0.2312
Power Factor	0.8414	0.8552	0.8799	0.8700	0.8700	0.8699

<sup>a</sup>Active power demand in [per-unit].

participated in the DLC program (load curtailment program) according to Table 4 where the corresponding power factor remains constant. In fact, in this test, the OPF based on the load curtailment program with a priority list is implemented. In this case, unlike section 4.1, because of the various load curtailment cost and priority list, we chose the cost coefficients of virtual generators according to Table 5, differently.

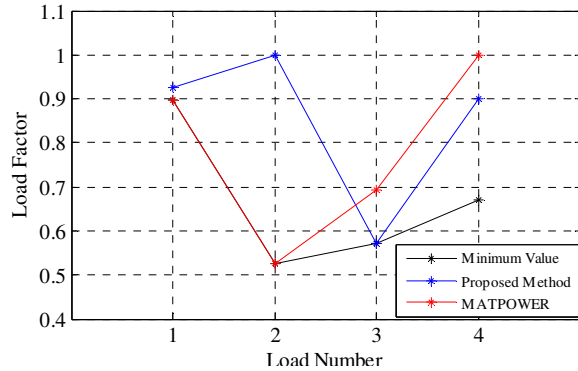


Fig. 7. Load factor of participated loads (IEEE 14-bus system).

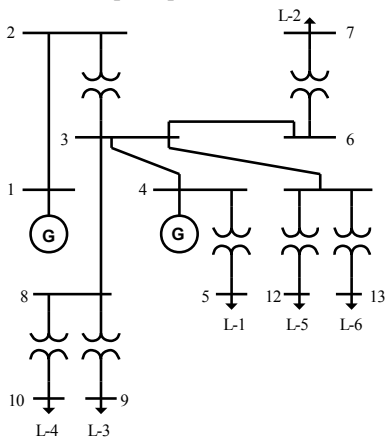


Fig. 8. 13-node industrial power system.

Table 5. Cost coefficients of virtual generators of 13-node industrial power system.

Bus No.	5	7	9	10	12	13
$\alpha^a$	0.5	0.5	0.5	0.5	0.5	0.5
$\beta^b$	20.7	20.4	20.5	20.6	20.8	20.3
Position in the Priority List	5	2	3	4	6	1

<sup>a</sup> All in [ $\$/\text{per-unit}^2 \cdot \text{h}^{-1}$ ], <sup>b</sup> All in [ $\$/\text{per-unit} \cdot \text{h}^{-1}$ ].

Table 6. Optimal power generations of 13-node industrial power system.

		$P_{g1}^a$	$P_{g2}$	$Q_{g1}$	$Q_{g2}$	Total Cost <sup>b</sup>
Without DLC <sup>c</sup>		0.549	0.094	-0.022	0.431	-
With DLC	Proposed	0.352	0.256	-0.010	0.386	32.62
	MATPOWER	0.351	0.195	-0.012	0.348	34.32

<sup>a</sup> All in [per-unit], <sup>b</sup> All in [ $\$/\text{h}^{-1}$ ], <sup>c</sup> This solution is not feasible.

The optimal solution for this case is obtained applying the proposed method and MATPOWER. The results are shown in Table 6. As it can be observed from this table, the proposed method limits the active power generations to their upper bounds which the objective function value is 32.62 ( $\$/\text{h}$ ). The optimal load curtailments are shown in Fig. 9 where only loads at bus 7 (L-2) and 13 (L-6) reduced by 1.13 % and 12.75 %, respectively.

In this regard, MATPOWER proposes a different operating point as shown in Table 6 and Fig. 9. The active power production reduced by 9.70 %, in comparison with results obtained by the proposed approach. But, for all loads, it uses the maximum possible load curtailment. Total cost obtained using MATPOWER is 34.32 ( $\$/\text{h}$ ).

It should be noted that the solution without DLC program is not feasible; because the active power generation by the first thermal unit is violated.

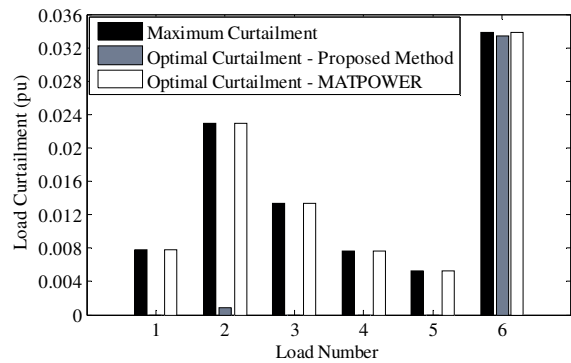


Fig. 9. Results of implementation load curtailment program on 13-node system.

The voltage profiles are shown in Fig. 10 and can be observed that all voltage buses remain in the acceptable range. Also, the voltages do not change much. Fig. 11 illustrates the load factors of curtailed loads of 13-node power system. This figure shows that the load factors obtained using MATPOWER are fixed to minimum values. It is because of the fact that MATPOWER uses the maximum load shedding.

**4.3. Implementation of the DLC program and proposed methodology on IEEE 30-bus system as a larger test case**

IEEE 30-bus test system (Fig. 12) is a balanced one that has six generators where the corresponding buses are considered as PV ones.

It is assumed that the customers at buses 2, 7, 10, 12, 16, 19, 29 and 30 have accepted to participate in the load curtailment program according to Table 7, where their power factor remains constant. For this test case,  $\alpha_{ij}$  and  $\beta_{ij}$  are selected as 500 (\$/per-unit<sup>2</sup>·h<sup>-1</sup>) and 300 (\$/per-unit<sup>1</sup>·h<sup>-1</sup>) for all virtual generators, respectively.

The obtained optimal power production using the suggested algorithm is presented in Table 8 and compared with those obtained using MATPOWER. It can be observed that the obtained results are better than those of MATPOWER. After optimization process, the objective function values will be equal to 102.25 (\$/h) and 106.06 (\$/h) for the presented method and MATPOWER, respectively.

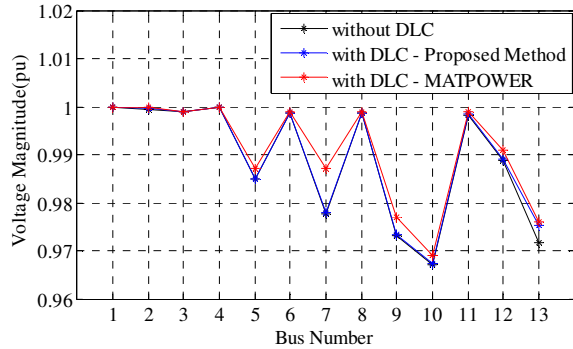


Fig. 10. Voltage profile of 13-node industrial system.

Table 7. Load curtailment characteristics of IEEE 30-bus test system.

Bus No.	2	7	10	12	16	19	29	30
Load No.	1	2	3	4	5	6	7	8
$P_{max}^a$	0.217	0.228	0.058	0.112	0.035	0.095	0.024	0.106
$P_{min}^a$	0.186	0.132	0.015	0.050	0.003	0.082	0.014	0.089
Power Factor	0.863	0.902	0.945	0.831	0.889	0.941	0.936	0.984

<sup>a</sup>Active power demand in [per-unit].

Table 8. Optimal power generations of IEEE 30-bus test system.

		$P_{g1}^a$	$P_{g2}$	$P_{g5}$	$P_{g8}$	$P_{g11}$	$P_{g13}$	$Q_{g1}$	$Q_{g2}$	$Q_{g5}$	$Q_{g8}$	$Q_{g11}$	$Q_{g13}$	Total Cost <sup>b</sup>
Without DLC		1.767	0.488	0.215	0.216	0.121	0.120	0.012	0.283	0.277	0.240	0.158	0.093	-
With DLC	Proposed	1.677	0.464	0.207	0.165	0.103	0.120	0.020	-0.513	0.299	0.254	0.153	0.083	102.25
	MATPOWER	0.500	0.447	0.150	0.331	0.100	0.120	0.562	-0.129	-0.150	0.274	0.209	0.113	106.06

<sup>a</sup>All in [per-unit]. <sup>b</sup>All in [\$·h<sup>-1</sup>].

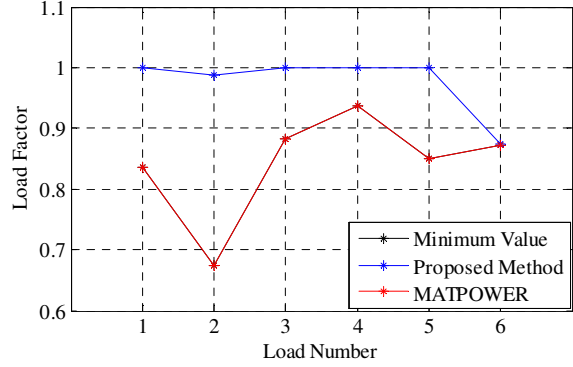


Fig. 11. Load factor of participated loads (13-node industrial system).

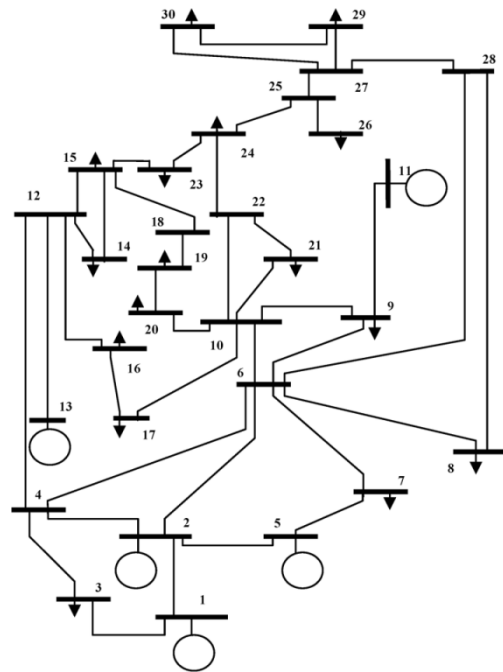


Fig. 12. IEEE 30-bus power system.

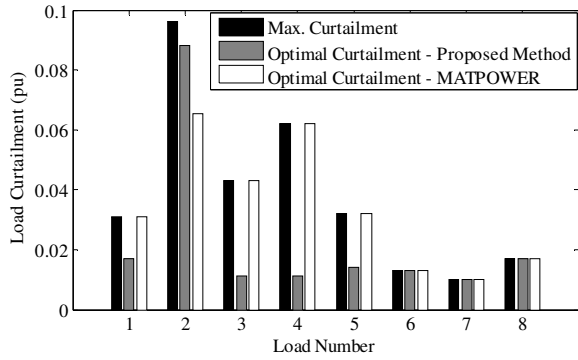


Fig. 13. Results of implementation load curtailment program on IEEE 30-bus system.

The optimal load curtailments are illustrated in Fig. 13. The results indicate that active demand reduced by 20.68 % and 31.23 % for the proposed algorithm and MATPOWER, respectively. In fact, MATPOWER shows more curtailing in comparison with the suggested approach.

Fig. 14 shows the voltage profiles of IEEE 30-bus power system with and without implementation of the load curtailment program. It can be observed that the voltage magnitudes are in the acceptable range. The load factors illustrate in Fig. 15 in which all factors show relative improvement in comparison with MATPOWER and minimum ones.

#### 4.4. Computational performances

The proposed methodology implemented in MATLAB 2009a [22] in the Windows 7 environment. The computational performances were evaluated on an Intel Pentium Dual Core Processor T3200, 2.0 GHz with 2.0 GB RAM PC. The results are summarized in Table 9.

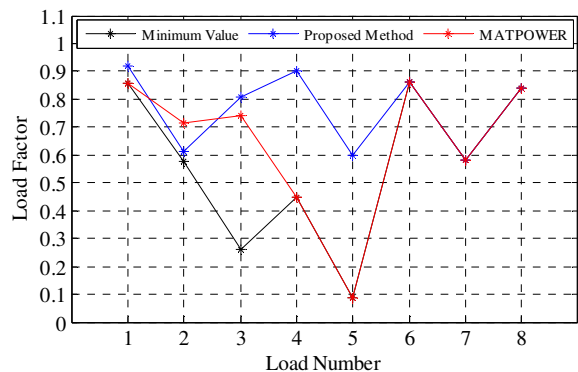


Fig. 15. Load factor of participated loads (IEEE 30-bus system).

As it can be observed from this table, for larger scale power systems, the number of iterations increases. This is more evident in the introduced approach. This conclusion is valid for average

computational times and is mainly because of the complexity of the equations in Eq. (14). In other words, the complexity of Eq. (14) grows as the number of transmission lines increases. Computational performances of MATPOWER show that the number of iterations remains constant, approximately.

### 5. CONCLUSIONS

In this paper, a new OPF methodology is proposed and combined with a novel load curtailment programs through the objective function. Also, the new load curtailment cost is proposed which have important advantages enable customers to participate in the DR programs. The methodology implemented on three balanced power systems as three smart grids under various scenarios and results in terms of quality solution and computational performances are compared with MATPOWER results and nominal case. The numerical results demonstrate that the proposed OPF limits the set of inequality constraints to their ranges, as well as the optimal operation of the smart grid is always obtained so that the quality solution is improved.

#### APPENDIX A

Selecting the constant parameter of  $s_i$   $(\max^{s_i(I_i(\mathbf{X}))}(0, I_i(\mathbf{X})))'$  changes from 1 to 0, quickly, when  $(I_i(\mathbf{X}) > 0) \rightarrow 0$ . Under this condition, the convergence rate may be slowly when  $x_i \in \mathbf{X}$  is far from the saddle-point. This means that the  $i$ th inequality constraint is out of the feasible region and  $x_i$  must be forced into the feasible region ( $i$ th inequality constraint must be satisfied). Then, for  $x_i$  away from minimum point where within the feasible region; but is out of it,  $s_i$  must be greater. So, for  $x_i$  near the boundary of the feasible region,  $s_i$  is very close to 1, and causes  $x_i$  almost reaches to its limits exactly. For fast convergence, we considered 3 points as:

- 1) If  $I_i(\mathbf{X}) \rightarrow 0$ , then  $s_i \rightarrow \frac{\alpha_2}{\alpha_5} = 1.25$
- 2) If  $I_i(\mathbf{X}) \rightarrow 1$ , then  $s_i \rightarrow \frac{\alpha_0 + \alpha_1 + \alpha_2}{\alpha_3 + \alpha_4 + \alpha_5} \cong 2$
- 3) If  $I_i(\mathbf{X}) \gg 1$ , then  $s_i \rightarrow \frac{\alpha_0}{\alpha_3} = 2.5$

We chose  $\alpha_0$ ,  $\alpha_3$ , and  $\alpha_5$  and obtain  $\alpha_1$ ,  $\alpha_2$ , and  $\alpha_4$  from the above points. The results are

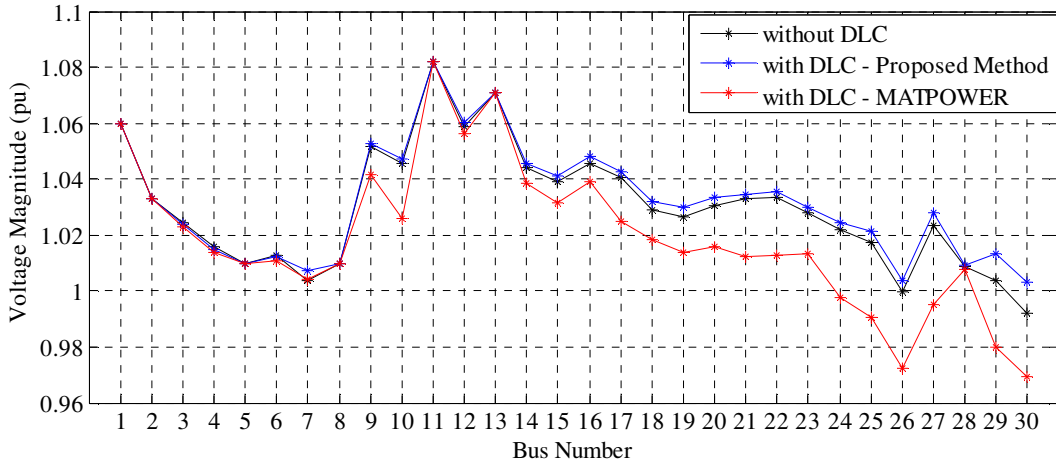


Fig. 14. Voltage profile of IEEE 30-bus power system.

Table 9. Computational performances.

Case Study	Avg. CPU time [s]		Iteration	
	Proposed Method	MATPOWER	Proposed Method	MATPOWER
13-node Industrial System	0.632	1.087	6	12
IEEE 14-bus System	1.177	1.201	10	13
IEEE 30-bus System	1.792	1.421	28	13

Table 10. Cost coefficients and power generation bus data for IEEE 14-bus test system.

Bus No.	1	2	3	6	8
$\alpha$ [\$/ (per-unit <sup>2</sup> ·h)]	50	50	-	-	-
$\beta$ [\$/ (per-unit·h)]	245	351	-	-	-
$\gamma$ [\$/h]	12	26	-	-	-
$P_{min}$ [per-unit]	0.3	0.4	-	-	-
$P_{max}$ [per-unit]	1.9	1.2	-	-	-
$Q_{min}$ [per-unit]	-	-0.4	0	-0.06	-0.06
$Q_{max}$ [per-unit]	-	0.5	0.4	0.24	0.24
Voltage Magnitude [per-unit]	1.060	1.045	1.010	1.070	1.090

summarized in Table 1.

**APPENDIX B**

**MATPOWER package**

MATPOWER is an open-source MATLAB-based power system simulation package that provides a high-level set of power flow, OPF, and other tools targeted toward researchers, educators, and students. The OPF architecture is designed to be extensible, making it easy to add user-defined variables, costs, and constraints to the standard OPF problem. This package consists of a set of MATLAB M-files designed to give the best performance possible while keeping the code simple to understand and customize [12]. In order to print output to the screen, which it does by default, `runopf` optionally returns

the solution in output arguments:

```
>> [baseMVA, bus, gen, gencost, branch, f, success, et] = runopf(casename)
```

In this paper, for comparison purpose, OPF-based load curtailment scenarios are performed using modified MATPOWER functions.

**APPENDIX C**

**Power generation bus data for IEEE 14-bus system**

The data are on 100 MVA base (Table 10).

**APPENDIX D**

**System data for 13-node industrial test system**

The data are on 10 MVA base (Table 11-13).

**Table 11.** Cost coefficients and power generation limits for 13-node industrial power system.

Bus No.	1	2
$\alpha$ [\$/per-unit <sup>2</sup> -h]	0.5	0.4
$\beta$ [\$/per-unit-h]	24.5	25.1
$\gamma$ [\$/h]	15	16
$P_{min}$ [per-unit]	0	0
$P_{max}$ [per-unit]	see section 4.2	
$Q_{min}$ [per-unit]	-0.2	-0.2
$Q_{max}$ [per-unit]	0.8	0.8

**Table 12.** Bus data for 13-node industrial power system.

Bus No.	Bus Voltage		Load <sup>a</sup>	
	Magnitude <sup>a</sup>	Phase Angle <sup>b</sup>	Active	Reactive
1	1.000	0	0	0
2	-	-	0	0
3	-	-	0	0
4	1.000	-	0	0
5	-	-	0.0478	0.0307
6	-	-	0	0
7	-	-	0.0703	0.0426
8	-	-	0	0
9	-	-	0.0963	0.0520
10	-	-	0.1237	0.0701
11	-	-	0	0
12	-	-	0.0353	0.0200
13	-	-	0.2650	0.1502

<sup>a</sup>All in [per-unit].<sup>b</sup>All in [deg].

**Table 13.** Line data for 13-node industrial power system.

Line No.	From Bus	To Bus	Line Impedance <sup>a</sup>		Y <sup>b</sup>
			Resistance	Reactance	
1	1	2	0.00139	0.00296	0.0048
2	2	3	0.00313	0.05324	0
3	3	4	0.00122	0.00243	0
4	4	5	0.06391	0.37797	0
5	3	6	0.00157	0.00131	0
6	6	7	0.05829	0.37888	0
7	3	8	0.00075	0.00063	0
8	8	9	0.05918	0.35510	0
9	8	10	0.04314	0.34514	0
10	3	11	0.00109	0.00091	0
11	11	12	0.05575	0.36240	0
12	11	13	0.01218	0.14616	0

<sup>a</sup>All in [per-unit].<sup>b</sup>Susceptance in [per-unit].

**REFERENCES**

[1] M. Allahnoori, Sh. Kazemi, H. Abdi and R. Keyhani, "Reliability assessment of distribution

systems in presence of microgrids considering uncertainty in generation and load demand," *Journal of Operation and Automation in Power Engineering*, vol. 2, no. 2, pp. 113–120, 2014.

[2] F. Rahimi, and A. Ipakchi, "Demand Response as a market resource under the smart grid paradigm," *IEEE Transactions on Smart Grid*, vol. 1, no. 1, pp. 82–88, 2010.

[3] U.S. Department of Energy, "Benefits of demand response in electricity markets and recommendations for achieving them," *Technical Report*, U.S. DOE, 2006.

[4] Sh. Lin and J. Chen, "Distributed optimal power flow for smart grid transmission system with renewable energy sources," *Energy*, vol. 56, pp. 184-192, 2013.

[5] S. Bruno, S. Lamonaca, G. Rotondo, U. Stecchi, and M.L. Scala, "Unbalanced three-phase optimal power flow for smart grids," *IEEE Transactions on Industrial Electronics*, vol. 58, no. 10, pp. 4504-4513, 2011.

[6] S. Paudyal, C.A. Cañizares and K. Bhattacharya, "Optimal operation of distribution feeders in smart grids," *IEEE Transactions on Industrial Electronics*, vol. 58, no. 10, pp. 4495-4513, 2011.

[7] Y. Levron, J.M. Guerrero, and Y. Beck, "Optimal power flow in microgrids with energy storage," *IEEE Transactions on Power Systems*, vol. 28, no. 3, pp. 3226-3234, 2013.

[8] T. Erseghe, and S. Tomasin, "Power flow optimization for smart microgrids by SDP relaxation on linear networks," *IEEE Transactions on Smart Grid*, vol. 4, no. 2, pp. 751-762, 2013.

[9] E.D. Anese, H. Zhu and G.B. Giannakis, "Distributed optimal power flow for smart microgrids," *IEEE Transactions on Smart Grid*, vol. 4, no. 3, pp. 1464-1475, 2013.

[10] L.R. Araujo, D.R.R. Penido, and F.A. Vieira, "A multiphase optimal power flow algorithm for unbalanced distribution systems," *International Journal of Electrical Power & Energy Systems*, vol. 53, pp. 632-642, 2013.

[11] *IEEE Recommended Practice for Industrial and Commercial Power Systems Analysis*, IEEE Standard 399, 1998.

[12] R.D. Zimmerman, C.E. Murillo-Sánchez and R.J. Thomas, "MATPOWER: steady-state operations, planning and analysis tools for power systems research and education," *IEEE Transactions on Power Systems*, vol. 26, no. 1, pp. 12-19, 2011.

[13] H.A. Aalami, M. Parsa Moghaddam and G.R. Yousefi, "Demand response modeling considering interruptible/curtailable loads and capacity market programs," *Applied Energy*, vol. 87, no. 1, pp. 243-250, 2010.

[14] North American Electric Reliability Corporation Reliability Assessment Subcommittee, "Demand response discussion for the 2007 long-term reliability assessment," *Technical Report*, 2007.

- [15] U.S. Department of Energy, "Assessment of demand response and advanced metering," *Technical Report*, 2006.
- [16] M.H. Albadi, and E.F. El-Saadany, "A summary of demand response in electricity markets," *Electric Power Systems Research*, vol. 78, no. 11, pp. 1989-1996, 2008.
- [17] J.R. Stitt, "Implementation of a large-scale direct load control system-some critical factors," *IEEE Transactions on Power Apparatus and Systems*, vol. PAS-104, no. 7, pp. 1663-1669, 1985.
- [18] A. Mohd, E. Ortjohann, A. Schmelter, N. Hamsic, and D. Morton, "Challenges in integrating distributed energy storage systems into future smart grid," *Proceedings of the IEEE International Symposium on Industrial Electronics*, pp. 1627-1632, 2008.
- [19] A.J. Wood and B.F. Wollenberg, *Power Generation, Operation & Control*, Wiley-Interscience, 1996.
- [20] S.S. Murthy, B. Singh and V. Sandeep, "A novel and comprehensive performance analysis of a single-phase two-winding self-excited induction generator," *IEEE Transactions on Energy Conversion*, vol. 27, no. 1, pp. 117-127, 2012.
- [21] M.H. Haque, "A novel method of evaluating performance characteristics of a self-excited induction generator," *IEEE Transactions on Energy Conversion*, vol. 24, no. 2, pp. 358-365, 2009.
- [22] MATLAB R2009a and Simulink, The MathWorks, Inc., 2009.
- [23] D.G. Luenbberger, *Linear and Nonlinear Programming*, Addison-Wesley, 1984.
- [24] T. Wang, and B.W. Wah, "Handling inequality constraints in continuous nonlinear global optimization," *Integrated Design and Process Science*, pp. 267-274, 1996.